Int. J. Electrochem. Sci., 13 **(2018)** 11730 – 11740, doi: 10.20964/2018.12.76

International Journal of
ELECTROCHEMICAL
SCIENCE
www.electrochemsci.org

Low-potential Electrosynthesis and Fluorescence Properties of Poly(9,9'-bifluorenylidene) in Boron Trifluoride Diethyl Etherate

Nannan Jian[1], *Wenna Zhang*[2], *Kai Qu*[1], *Shuai Chen*[2], *Baoyang Lu*[2,*], *Ximei Liu*[2,*], *Jingkun Xu*[1,3,*]

[1] School of Chemistry & Chemical Engineering, Jiangxi Science & Technology Normal University, Nanchang 330013, Jiangxi, China
[2] School of Pharmacy, Jiangxi Science & Technology Normal University, Nanchang 330013, Jiangxi, China
[3] School of Chemistry and Molecular Engineering, Qingdao University of Science and Technology, Qingdao 266042, Shandong, China
[*]E-mail: lby1258@163.com and xujingkun1971@yeah.net

Received: 14 August 2018 / *Accepted:* 12 October 2018 / *Published:* 5 November 2018

Electrosynthesized polyfluorene-based conjugated polymers (PFs) have been extensively researched since their discovery owing to their excellent fluorescence properties and one step fabrication process. However, most polyfluorenes have been obtained under high polymerization potentials over 1.2 V vs. Ag/AgCl, resulting in inevitable overoxidation and structural defects of the deposited polymer films, and thus imposing instability and long-term deterioration in optoelectronic properties. Herein, by the employment of a fused 9,9'-bifluorenylidene (BFY) as the initial monomer and boron trifluoride diethyl etherate (BFEE) as both the solvent and supporting electrolyte for the electropolymerization, we successfully achieved the low potential electrodeposition of a novel polyfluorene film for the first time at 0.9 V vs. Ag/AgCl. We demonstrate that the polymerization mechanism of BFY occurs dominantly at the 2,7 positions of the fluorene unit and forms an interconnected network of polyfluorene segments. The electropolymerization of BFY displays a sphere-type deposition process to produce a surface morphology of nanosphere clusters. We further explore the thermal degradation and electronic property evolution from monomer BFY to the deposited polymer, and find that the polymer exhibits a 100 nm-red shift in electronic absorption and significantly enhanced fluorescence intensity with a high quantum yield up to 0.78.

Keywords: conjugated polymers, electropolymerization, 9,9'-bifluorenylidene, boron trifluoride diethyl etherate, fluorescence

1. INTRODUCTION

With the development of electroactive and photoactive materials over the last two decades,[1-3] polyfluorene-based conjugated polymers (PFs) (**Scheme 1**) have received a great deal of attention as one of the most important blue light-emitting materials.[4-8] For the preparation of such materials, electrochemical polymerization is an effective method to achieve high-performance polyfluorenes owing to several advantages such as one-step film electrodeposition without using catalysts/oxidants, ease of fabricating electronic devices/sensors, free of complex materials processing procedures, and so on.[9.10] Previously mono- and di-substituted PFs (**Scheme 1**) at C-9 position with different kinds of functional groups have been synthesized via electropolymerization and their photoelectronic properties have been investigated in detail.[11-14] However, most electropolymerized polyfluorenes have been obtained under high polymerization potentials over 1.2 V vs. Ag/AgCl, resulting in inevitable overoxidation and structural defects of the deposited polymer films, and thus imposing instability and long-term deterioration in optoelectronic properties.

Electrolytes are proved to significantly influence the electropolymerization process and performances of electrosynthesized PFs films. Previously reported PFs films electrosynthesized in common organic solvents are usually unstable, brittle and insoluble, ascribed to the excessively high applied potential which can destroy the conjugated structures of polymers.[15-20] From the materials development perspective, reducing the onset oxidation potential is a crucial factor for achieving high-performance polymer films via electropolymerization. Our group[21,22] previously reported a variety of high-quality PFs polymers, which are obtained via the electropolymerization in pure boron trifluoride diethyl etherate (BEFF) or mixed solvent systems of BFEE and traditional solvents (**Scheme 1**). These homopolymers show reversible redox activity, outstanding electroactive and thermal stability, and excellent blue to green light-emitting properties. Therefore, BFEE is an superior electrolyte-solvent system for electropolymerization.[23] In the previous studies,[10,13,16,17,] the emphasis of PFs is the modification of C9-site with saturated alkanes groups, carboxylic acids, alcohols, and halogen atoms (**Scheme 1**), but no studies have been devoted to the electropolymerization of fused fluorene derivatives and the properties of as-formed PFs.

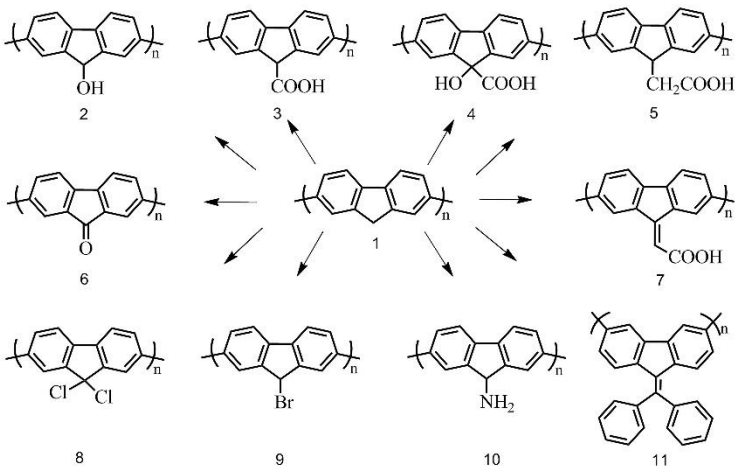

Herein, we study the electropolymerization of 9,9'-bifluorenylidene (BFY), a fused fluorene derivative with larger conjugated structure, planarity in BFEE. Its polymer, poly(9,9'-bifluorenylidene) (PBFY), is successfully achieved for the first time under optimized electrical condictions. The electropolymerization behavior of BFY, and the structure characterizations, surface morphology, optical properties, thermal stability, together with the fluorescence performances of PBFY, are studied and discussed in detail.

2. EXPERIMENTAL SECTION

2.1 Chemicals

9,9'-Bifluorenylidene (BFY, 99%; Acros Organics) was employed as the initial monomer and was used directly without any purification. BFEE (1.12~1.14 g mL^{-1}, BF_3 = 48.24%; Acros Organics) was used as both the solvent and supporting electrolyte for the electropolymerization and was distilled under a nitrogen atmosphere before use. Dichloromethane (CH_2Cl_2, 99.9%, superdry, with molecular sieves, J&K) was used as the solvent for the electropolymerization and used directly without any further treatment. Tetrabutylammonium tetrafluoroborate (Bu_4NBF_4, 99%, Energy) was dried under vacuum at 60 ºC for 24 h before use. ITO-coated glass (ITO-P005, R_{sh} < 15 Ω/□) was purchased from Zhuhai Kaivo Co., Ltd.

2.2 Characterization

The Bruker Vertex 70 Fourier-transform Infrared (FT-IR) spectrometer was used to record the structures of the monomer and polymer. The surface morphology of the dedoped/doped polymer film deposited on the ITO-coated glass was investigated via a VEGA II-LSU scanning electron microscope (SEM, Tescan). The UV–vis spectra of the BFY and PBFY in CH_2Cl_2 were obtained by employing a Perkin-Elmer Lambda 900 Ultraviolet-visible Near-Infrared spectrophotometer. Fluorescence spectra in CH_2Cl_2 were recorded by an F-4500 fluorescence spectrophotometer (Hitachi) with the excitation and emission slit set at 5 nm. Thermogravimetric analysis (TGA) was performed with a Pyris Diamond TG/DTA thermal analyzer (Perkin-Elmer) at the heating rate 10 ºC min^{-1} under nitrogen atmosphere. The DFT calculations of the molecular geometries and frontier molecular orbtial distributions (HOMO and LUMO) of 9,9'-bifluorenylidene were carried out by using the Gaussian 09 program package under the B3LYP/6-31G(d, p) level.

2.3 Electrosynthesis and electrochemical tests

All the electrochemical experiments were controlled under Model 263A potentiostat-galvanostat (EG&G Princeton Applied Research) with the potential scan rate of 100 mV s^{-1}. In order to eliminate the effect of oxygen, the electrolyte system was bubbled by nitrogen for 30 min before experiments. Pt wires (diameter: 1 mm) were used as working and counter electrodes, and the

reference electrode was an Ag/AgCl electrode (diameter: 1 mm). In order to obtain enough polymers, the ITO-coated glass sheet (2 × 1.5 cm^2) was used as working electrode and Pt sheet (2 × 2 cm^2) was employed as the counter electrode. The polymer film was grown potentiostatically at the optimized potential in BFEE and the thickness was controlled by the total charge passed through the cell, which can be read directly from current-time (I-t) curves. After polymerization, the polymer film was washed repeatedly with CH_2Cl_2 to remove the electrolyte, monomer, and oligomer.

3. RESULTS AND DISCUSSION

3.1 Electrochemical polymerization of 9,9'-bifluorenylidene

The electropolymerization performances of BFY in CH_2Cl_2-Bu_4NBF_4 (0.1 mol L^{-1}) and BEEF have been investigated (**Fig. 1)**. The onset oxidation potential of BFY in CH_2Cl_2-Bu_4NBF_4 is approximately at 1.25 V vs. Ag/AgCl (**Fig. 1a**), which is consistent with the previously reported results.[21,24] During the cyclic voltammetry scanning, neither obvious redox waves nor polymers can be observed on the working electrode (**Fig. 1A**), indicating that the electropolymerization of BFY is impossible in CH_2Cl_2-Bu_4NBF_4 (0.1 mol L^{-1}) because of its high onset oxidation potential. Therefore, the CH_2Cl_2–Bu_4NBF_4 electrolyte is not the right choice for the electropolymerization of BFY.

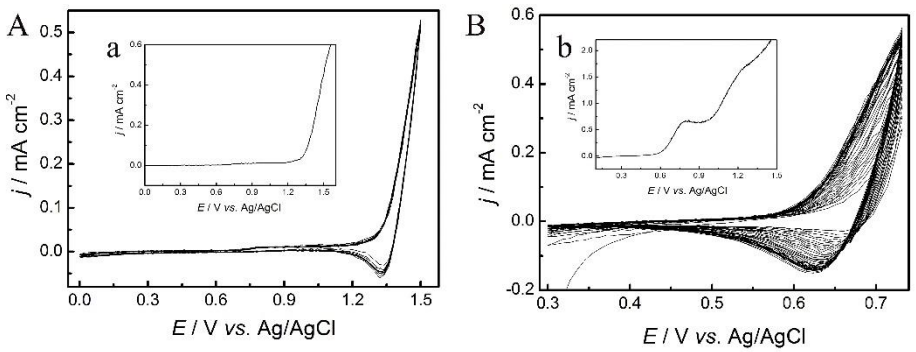

Figure 1. Cyclic voltammograms of 0.01 mol L^{-1} BFY in CH_2Cl_2-Bu_4NBF_4 (0.1 mol L^{-1}) (A) and in BFEE (B). Inset: Anodic polarization curves of 0.01 mol L^{-1} BFY in CH_2Cl_2-Bu_4NBF_4 (0.1 mol L^{-1}) (a) and in BFEE (b). Potential scan rate: 100 mV s^{-1}.

Considering its catalytic effect on the decrease of the onset oxidation potentials for aromatic compounds,[25-27] BFEE was chosen as both the solvent and electrolyte (without any other additives) for the electropolymerization of BFY. The onset oxidation potential of BFY is obviously reduced to 0.70 V vs. Ag/AgCl (**Fig. 1b)**, much lower than that in CH_2Cl_2-Bu_4NBF_4 (0.1 mol L^{-1}) (1.25 V), due to the interaction between the BFEE and aromatic BFY monomer. Generally speaking, the monomer with high onset oxidation potential is quite difficult to electropolymerize and even leads to some side reactions in the electropolymerization process, such as overoxidation.[28] Moreover, the redox peak current densities increasing with the successive potential scanning process (**Fig. 1B**), indicating that

the polymer film increased simultaneously on the surface of the working electrode. Meanwhile, the redox peaks become broad, which can be attributed to the improvement of the polymer quality and the elongation of the polymer chains.

3.2 Optimization of electrochemical conditions and preparation of PBFY

The electrochemical conditions such as polymerization potentials applied in the electropolymerization process directly affect the structure and properties of as-formed polymer film.[29] In order to find the optimal applied potential, a set of current transients at different applied potentials in BFEE have been investigated (**Fig. 2**). Below the onset oxidation potential, no polymers are deposited on the surface of the electrode, whereas too high potential will result in the overoxidation of the polymers, making them easily fall off the working electrode. By considering various factors including the regularity of the polymers, film adhesion on the working electrode, and polymerization rate and side reactions, the optimal applied potential of the BFY in BEFF is chosen as 1.0 V vs. Ag/AgCl. Thus, the following characterization tests of the polymer film are carried out under the constant potential. Under the optimal applied potential of 1.0 V vs. Ag/AgCl, the electropolymerization rate is moderate (**Fig. 2)**, which might effectively avoid the oxidation and control the thickness of the polymer film. Also, the film obtained is smooth and homogeneous. The onset oxidation potential and the optimal applied potential of the BFY is lower than the parent structure of fluorene, resulting from more delocalized conjugated structure and planarity.

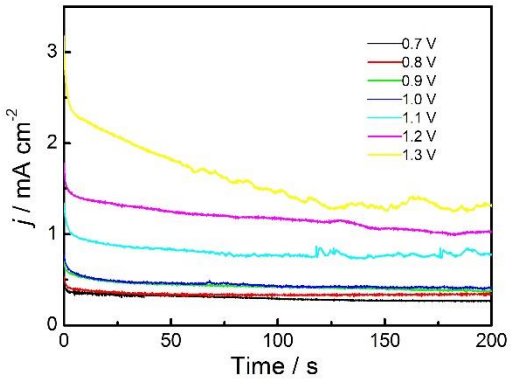

Figure 2. Chronoamperograms of 0.01 mol L^{-1} BFY in BFEE on Pt electrode at different applied potentials.

3.3 DFT theoretical calculations

The optimized geometry and HOMO and LUMO orbital distribution of the monomer, together with the electron spin density (ESD) for BFY radical cation are calculated by DFT calculations, as depicted in **Fig. 3**. It can be seen that most of the highest occupied molecular orbital (HOMO) are concentrated on C(2) and C(7) positions of the fluorene rings in BFY structure. Electron spin density of its radical cation demonstrates that the most active sites of the radical cation are also the C(2) and

C(7) positions of the fluorene rings. According to the molecular orbital theory and the radical cation mechanism for electropolymerization, the polymerization reaction among BFY monomers happens preferentially at these positions.

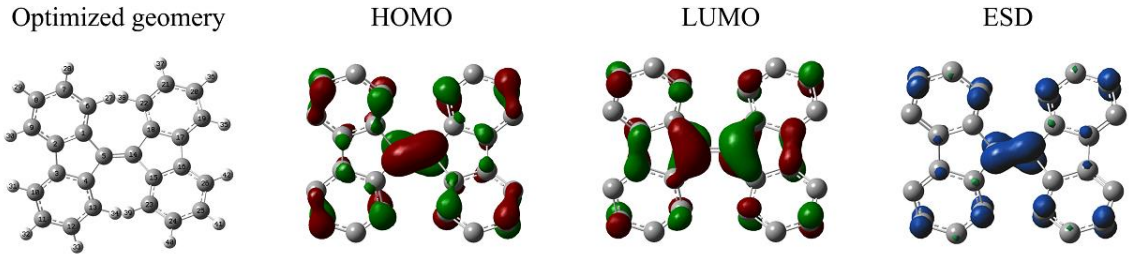

Figure 3. Optimized geometry and HOMO-LUMO distribution of BFY and electron spin density (ESD) for the corresponding radical cation.

3.4 Structural characterization

FI-IR spectra (**Fig. 4**) have been studied to explain the electropolymerization mechanism of BFY. The absorption peaks of the PBFY are obviously wider than those of BFY due to the longer conjugated chains of the polymers.[22] The absorption peaks from 1704 to 1610 cm^{-1} are attributed to the C=C stretching vibration of BFY (**Fig. 4A**). In the near-infrared region (1730~1597 cm^{-1}, **Fig. 4B**), a large amount of vibrational peaks of PBFY are observed. The C–H wagging vibration on the aromatic rings of the PBFY is extended to 1447~666 cm^{-1}. BFY display three peaks in 768-708 cm^{-1}, demonstrating the existence of the 1,2-disubstituted phenyl ring.[30,31] For PBFY, these peaks shift to 918-811 cm^{-1}, which are characteristic for the 1,2,4-trisubstituted phenyl ring. From these results, we can find that the polymerization of BFY dominantly happens on 2,7 positions of the fluorenyl rings, in good agreement with DFT calculation results.

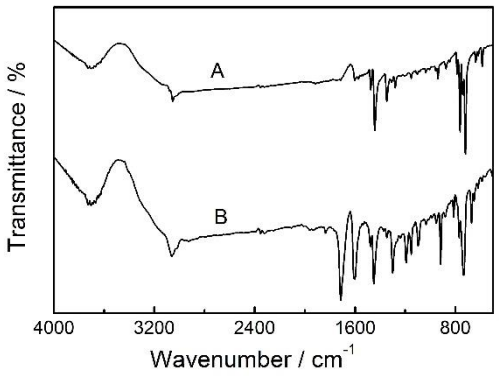

Figure 4. FI-IR spectra of BFY (A) and dedoped PBFY (B).

Due to the symmetrical structure of the BFY monomer, there may be four different polymeric structures: linear polymers with pendant monomer (**Scheme 2a)**, a ladder polymer (**Scheme 2b)**, linear polymers (**Scheme 2c)** and reticular polymer via randomly bridged method (**Scheme 2d)**. These four

kinds of polymer bridging structures can be obtained at low voltage through the catalytic polymerization of the BFEE. Considering the steric hindrance and the FT-IR results, the reticular polymer structure is the most reasonable way for the electropolymerization of BFY to form a interconnected network.

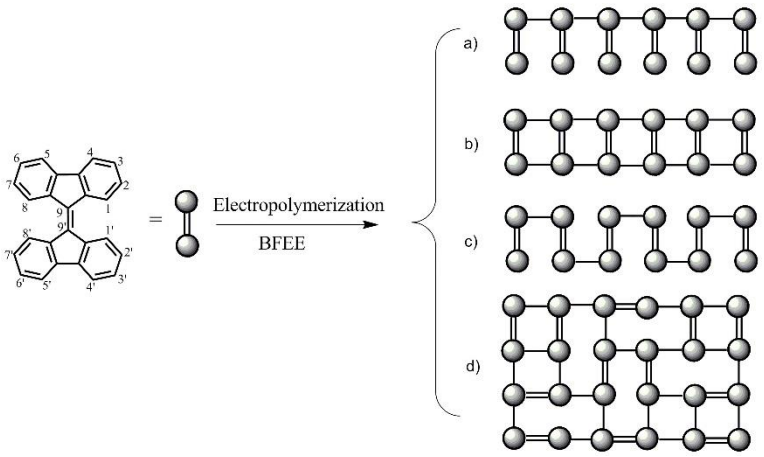

Scheme 2. Formation of different polymeric structures from precursors via electropolymerization in BFEE solution containing 0.01 mol L^{-1} BFY.

3.4 Morphology of the PBFY film

Surface morphology, which is closely related to the optical and electronic properties and usually investigated via scanning electron microscope (SEM), is a significant performance of the polymers. In this work, the surface morphology of the PBFY film deposited on the ITO glass have been investigated (**Fig. 5)**. There is an obvious difference between the doped (**Fig. 5A**) and dedoped (**Fig. 5B**) PBFY film. Concretely, under the doped state, the PBFY film shows sphere-type growth processes whereby a number of clusters (**Fig. 5A)**. This growth mode is a feature of stronger interactions between deposited molecules than between the film and substrate.[32] This morphology facilitates the immigration/emigration of counter anions, which is in good consistence with the redox activity of PBFY film. Note that the spheres of the dedoped PBFY film (**Fig. 4B**) are partially destroyed, probably resulting from the moving in/out of counter anions and the gradual solubility of PBFY film during the doping-dedoping processes. Compared with the surface morphology of the polyfluorene, PBFY film display a more smooth and homogeneous morphology. We hypothesize that the spatial connectivity of PBFY is most likely the network or the ladder rather than the linear type (**Scheme 2**). In term of this case, PBFY polymers with this structure can be used as new carriers in other fields, such as biology and catalysis.

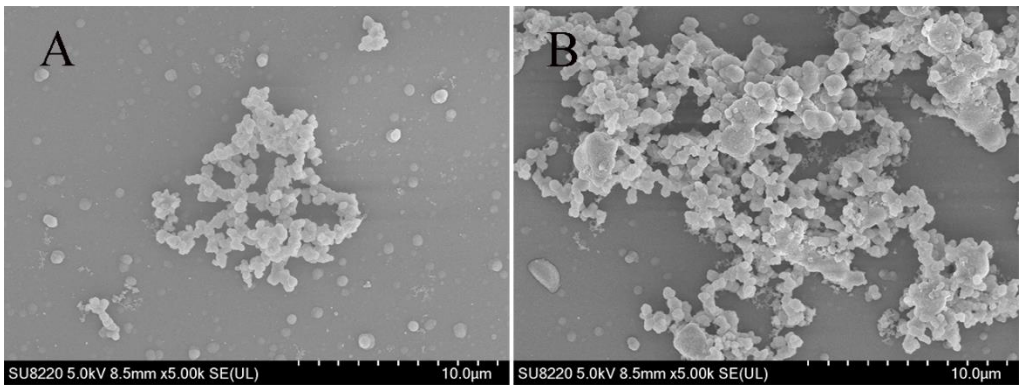

Figure 5. SEM images of doped (A) and dedoped (B) PBFY film deposited on the ITO electrode.

3.5 Thermal properties of PBFY

The thermal gravimetric analysis (TGA) with the temperature changes from 300 to 1000 K has been recorded to investigate the degradation behavior of PBFY (**Fig. 6)**. At low temperature (T < 400 K), PBMY initially loss weight about 0.2%, mainly due to the escape of the water vapor in the polymer. During the temperature changed from 430 to 700 K, the weight of the polymer is rapidly reduced by 70%. Meanwhile, the DTG curve of the polymer show the corresponding maximal decomposition at 470 and 600 K, attributed to the oxidizing decomposition of skeletal chain structure of the polymer. The weight loss after 700 K is closely related to the overflow of some structural fragments decomposed from PBFY previously. This is in good accordance with previous hypothesis for the interconnected network structure of PBFY, which is easily degraded into low molecular segments and flows out upon heating.

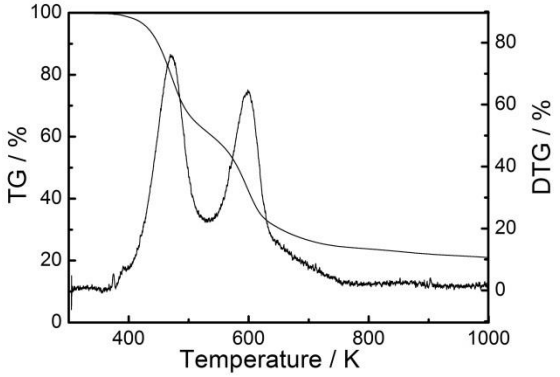

Figure 6. TG and DTG curves of PBFY.

3.6 Optical properties

The UV-vis spectra of the BFY and PBFY in CH_2Cl_2 have been investigated (**Fig. 7)**. An obvious and characteristic absorption peak of BFY at 350 nm can be observed (**Fig. 7A**) from the π–π* transition of the aromatic rings. Compared with BFY, the absorption peak of PBFY is distinctly broadened and red-shifted to 460 nm (**Fig. 7B** and **7C**), producing a 110 nm red shift. This is mainly attributed to the longer conjugated chains of PBFY compared to monomers.[33] These results confirm

that the occurrence of the electrochemical polymerization among the monomers and the formation of the conjugated polymers with broad molar mass distribution. Interestingly, the absorbance intensity of doped PBFY is stronger than that of dedoped state, which also supported the different surface morphology at different doped states.

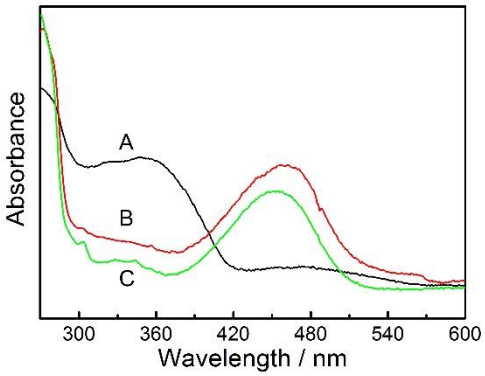

Figure 7. UV-visible spectra of BFY monomer (A), doped (B) and depoed (C) PBFY in CH_2Cl_2.

The fluorescence spectra of the BFY and PBFY in CH_2Cl_2 have been carefully determined (**Fig. 8)**. Interestingly BFY display no light-emission in CH_2Cl_2 in the range of 380-800 nm. This phenomenon is resulting from the tendency of BFY monomer to form stable free-radicals upon excitation. In contrast, a strong and wide peak centered at 480 nm characterize the emission spetrum of PBFY due to the prolonged π-conjugated structures. Interestingly, the precipitated oligo-/polymers in electrolyte system after electropolymerization display no light-emitting properties in both Et_2O and CH_2Cl_2 (**Fig. 8A & B**), ascribed to the ionized oligo-/polymers to form stable free-radical or ionic species. However, the electrosynthesized polymers peeling off the working electrode can emit strong and bright opalescent photoluminescence (exposed to the 365 nm UV light, **Fig. 9C & D**) with a very high quantum yield of 0.75 in Et_2O and 0.78 in CH_2Cl_2 (**Fig. 9D**). With these excellent fluorescence properties, PBFY can be a good candidate for utilization in energy saving lamp, polymer light-emitting diodes, fluorescent chemosensors, and so on.

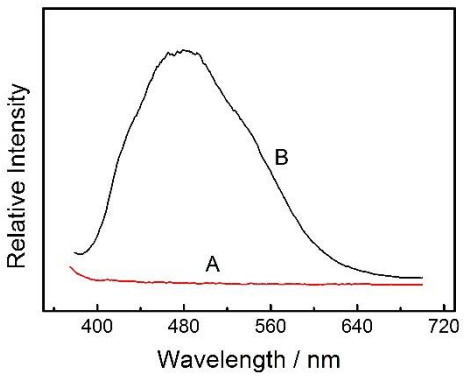

Figure 8. Photoluminescence and fluorescence spectra of BFY (A) and PBFY (B) in CH_2Cl_2.

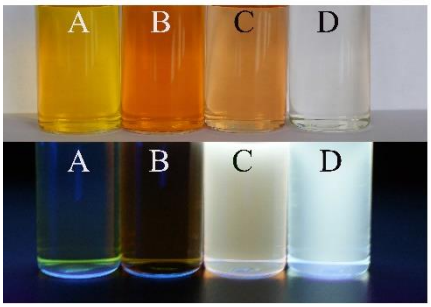

Figure 9. Photoluminescence of the precipitated oligo-/polymers extracted with Et_2O (A) and successively with CH_2Cl_2 (B); Photoluminescence of the electrosynthesized polymers peeling off the working electrode extracted with Et_2O (C) and successively with CH_2Cl_2 (D).

4. CONCLUSION

In this work, PBFY has been obtained for the first time via low potential electropolymerization with a fused fluorenyl monomer BFY and boron trifluoride diethyl etherate as both the solvent and supporting electrolyte at 0.9 V vs. Ag/AgCl. We demonstrate that the polymerization mechanism of BFY occurs dominantly at the 2,7 positions of the fluorene unit and forms an interconnected network of polyfluorene segments. The electropolymerization of BFY displays a sphere-type deposition process to produce a surface morphology of nanosphere clusters. We further explore the thermal degradation and electronic property evolution from monomer 9,9'-bifluorenylidene to the deposited polymer, and find that the polymer exhibits a 100 nm-red shift in electronic absorption and significantly enhanced fluorescence intensity with a high quantum yield up to 0.78. This material holds promise as the candidate for blue light-emitting materials and organic electronic devices.

ACKNOWLEDGEMENTS
This work was supported by the National Natural Science Foundation of China (51763010, 51863009), Innovation Driven “5511” Project of Jiangxi Province (20165BCB18016), Science Foundation for Excellent Youth Talents in Jiangxi Province (20162BCB23053), the Key Research and Development Program of Jiangxi Province (20171BBH80007, 20181ACB20010), the Natural Science Foundation of Jiangxi Province (20171BAB216018), and Science and Technology Foundation of Jiangxi Educational Committee (GJJ160790). N. J. thanks Jiangxi Science & Technology Normal University for a Postgraduate Innovation Program grant (YC2017-X26).

References

1. Y. Yan, S.L. Jiang, W.L. Zhou, X.S. Miao, Y.K. Zeng, G.Z. Zhang and S.S. Liu. *Sci. Rep.,* 3 (2013) 2697.
2. Z.W. Wang, Q. Zhang, K. Zhang and G. Hu, *Adv. Mater.*, 28 (2016) 9857.
3. Y. Sun, C.R. Qu, H. Chen, M.M. He, C. Tang, K.Q. Shou, S.H. Hong, M. Yang, Y.X. Jiang, B.B. Ding, Y.L. Xiao, L. Xing, X.C. Hong and Z. Cheng, *Chem. Sci.*, 7 (2016) 6203.
4. T. Fukumaru, F. Toshimitsu, T. Fujigaya and N. Nakashima, *Nanoscale*, 6 (2014) 5879.
5. T.Z. Yu, W.J. Guan, X. Wang, Y.L. Zhao, Q.G. Yang, Y.M. Li and H. Zhang, *New J. Chem.*, 42

(2018) 2094.
6. A.C. Grimsdale, K.L. Chan, R.E. Martin, P.G. Jokisz and A.B. Holmes, *Chem. Rev.*, 109 (2009) 897.
7. U. Scherf and E.J.W. List, *Adv. Mate*r., 14 (2002) 477.
8. B. Muthuraj, S. Mukherjee, C.R. Patra and P.K. Iyer, *ACS Appl. Mater. Interfaces*, 8 (2016) 32220.
9. L. Liu, K. Wu, J. Ding, B. Zhang and Z. Xie, *Polymer*, 54 (2013) 6236.
10. R.B. Aïch, N. Blouin, A. Bouchard and M. Leclerc, *Chem. Mater.*, 21 (2009) 751.
11. F.I. Wu, A.P. Shih, C.F. Shu, Y.L. Tung and Y. Chi, *Macromolecules*, 38 (2005) 9028.
12. L. He, L. Duan, J. Qiao, G.F. Dong, L.D. Wang and Y. Qiu, *Chem. Mater.*, 22 (2010) 3535.
13. N. Blouin, A. Michaud and M. Leclerc, *Adv. Mater.*, 19 (2007) 2295.
14. K.W. Lin, S. Chen, B.Y. Lu and J.K. Xu, *Sci. China Chem.*, 60 (2017) 38.
15. V.K. Gupta, M.R. Ganjali, P. Norouzi, H. Khani, A. Nayak and S. Agarwal, *Crit. Rev. Anal. Chem.*, 41 (2011) 282.
16. K. Bai, S. Wang, L. Zhao, J. Ding and L. Wang, *Macromolecules,* 50 (2017) 6945.
17. H.B. Wu, G.J. Zhou, J.H. Zou, C.L. Ho, W.Y. Wong, W. Yang, J.B. Peng and Y. Cao, *Adv. Mate*r., 21 (2010) 4181.
18. G. Klarner, J.I. Lee, M.H. Davey, and R.D. Miller, *Adv. Mater.*, 11 (1999) 115.
19. H.Y. Byun, I.J. Chung, H.K. Shim and C.Y. Kim, *Chem. Phys. Lett.*, 393 (2004) 197.
20. W. Chen and G. Xue, *Prog. Polym. Sci.*, 30 (2005) 783.
21. J.K. Xu, Z.H. Wei, Y.K. Du, W.Q. Zhou and S.Z. Pu, *Electrochim. Acta*, 51 (2006) 4771.
22. J.K. Xu, Y.J. Zhang, J. Hou, Z.H. Wei, S.Z. Pu, J.Q. Zhao and Y.K. Du, *Eur. Polym. J.*, 42 (2006) 1154.
23. C.Y. Zhang, Y.J. Tao, K. Zhang, H.F. Cheng and X.Q. Xu, *Opt. Mater.*, 75 (2018) 654.
24. J.R. Berthelot and M.M. Granger, *J. Electroanal. Chem.*, 353 (1993) 341.
25. C.L. Fan, J.K. Xu, W. Chen, B.Y. Lu, H.M. Miao, C.C. Liu and G.D. Liu, *J. Phys. Chem. C*, 113 (2009) 9900.
26. G.M. Nie, Q.F. Guo, Y. Zhang and S.S. Zhang, *Eur. Polym. J.*, 45 (2009) 2600.
27. S.S. Zhang, G.M. Nie, X.J. Han, J.K. Xu, M.S. Li and T. Cai, *Electrochim. Acta*, 51 (2006) 5738.
28. W.N. Zhang, W.W. Zhang, H.T. Liu, N.N. Jian, K. Qu, S. Chen and J.K. Xu, *J. Electroanal.Chem.*, 813 (2018) 109.
29. Z.L. Feng, D.Z. Mo, Z.P. Wang, S.J. Zhen, J.K. Xu, B.Y. Lu, S.L. Ming, K.W. Lin and J.H. Xiong, *Electrochim. Acta*, 160 (2015) 160.
30. J. Heinze, B.A. Frontanauribe and S. Ludwigs, *Chem. Rev.*, 110 (2010) 4724.
31. B.Y. Lu, J.Y. Wang, R.R. Yue, J.K. Xu and M.S. Pei, *J. Mater. Sci.*, 47 (2012) 315.
32. B.Y. Lu, J. Yan, J.K. Xu, S.Y. Zhou and X.J. Hu, *Macromolecules*, 43 (2010) 4599.
33. N.N. Jian, H. Gu, S.M. Zhang, H.T. Liu, K. Qu, S. Chen, X.M. Liu, Y.F. He, G.F. Niu, S.Y. Tai, J. Wang, B.Y. Lu, J.K. Xu and Y. Yu, *Electrochim. Acta*, 266 (2018) 263.